JOURNAL OF THE ROYAL SOCIETY Interface

Unsteady motion: escape jumps in planktonic copepods, their kinematics and energetics

Thomas Kiørboe, Anders Andersen, Vincent J. Langlois and Hans H. Jakobsen

J. R. Soc. Interface published online 12 May 2010
doi: 10.1098/rsif.2010.0176

JOURNAL OF THE ROYAL SOCIETY Interface

FirstCite® e-publishing

J. R. Soc. Interface
doi:10.1098/rsif.2010.0176
Published online

Unsteady motion: escape jumps in planktonic copepods, their kinematics and energetics

Thomas Kiørboe[1,*], Anders Andersen[2], Vincent J. Langlois[3] and Hans H. Jakobsen[1]

[1]*National Institute for Aquatic Resources, Technical University of Denmark, Kavalergården 6, 2920 Charlottenlund, Denmark*
[2]*Department of Physics and Center for Fluid Dynamics, Technical University of Denmark, 2800 Kgs Lyngby, Denmark*
[3]*Laboratoire de Sciences de la Terre, Université Claude Bernard Lyon 1-ENS Lyon-CNRS, 69622 Villeurbanne Cedex, France*

We describe the kinematics of escape jumps in three species of 0.3–3.0 mm-sized planktonic copepods. We find similar kinematics between species with periodically alternating power strokes and passive coasting and a resulting highly fluctuating escape velocity. By direct numerical simulations, we estimate the force and power output needed to accelerate and overcome drag. Both are very high compared with those of other organisms, as are the escape velocities in comparison to startle velocities of other aquatic animals. Thus, the maximum weight-specific force, which for muscle motors of other animals has been found to be near constant at 57 N (kg muscle)$^{-1}$, is more than an order of magnitude higher for the escaping copepods. We argue that this is feasible because most copepods have different systems for steady propulsion (feeding appendages) and intensive escapes (swimming legs), with the muscular arrangement of the latter probably adapted for high force production during short-lasting bursts. The resulting escape velocities scale with body length to power 0.65, different from the size-scaling of both similar sized and larger animals moving at constant velocity, but similar to that found for startle velocities in other aquatic organisms. The relative duration of the pauses between power strokes was observed to increase with organism size. We demonstrate that this is an inherent property of swimming by alternating power strokes and pauses. We finally show that the Strouhal number is in the range of peak propulsion efficiency, again suggesting that copepods are optimally designed for rapid escape jumps.

Keywords: hydrodynamics; startle response; muscle force; muscle power; escape velocity; Strouhal number

1. INTRODUCTION

Copepods constitute the absolutely dominating mesozooplankton group in marine plankton and are maybe the most abundant metazoans on the Earth (Humes 1994). Key to their success is probably their capability of detecting hydrodynamic disturbances created by approaching predators, and of escaping these at very high velocities (Verity & Smetacek 1996). Upon detecting a predator, millimetre-sized copepods may accelerate at more than 200 m s^{-2} and within milliseconds reach velocities of several hundreds of body lengths per second (Buskey *et al.* 2002; Lenz *et al.* 2004; Burdick *et al.* 2007; Waggett & Buskey 2007, 2008). Such escape jumps may bring the copepod to a safe distance from the predator. These traits are facilitated, respectively, by the sensory-armed antennae extending from the body and by a streamlined, muscular body-plan.

The size-scaling of swimming speed and limb movement frequency has been discussed at least since Hill (1950), who suggested that animals of similar shape should swim (or run) at size-independent velocities and that limb frequency should consequently scale inversely with length (Biewener 2003). In contrast, optimization of distance covered per unit of energy expenditure using constructural theory rather predicts that propulsion velocity should scale with the square root of organism length, and stroke frequency inversely with the square root of length in running, flying and swimming animals (Bejan & Marden 2006). Optimization considerations for propulsion efficiency lead to scaling properties that are consistent with either of these predictions (Taylor *et al.* 2003). These two theories mainly consider organisms operating at high

*Author for correspondence (tk@aqua.dtu.dk).

Electronic supplementary material is available at http://dx.doi.org/10.1098/rsif.2010.0176 or via http://rsif.royalsocietypublishing.org.

Received 22 March 2010
Accepted 20 April 2010

Reynolds numbers and moving at constant speed, and both theories have found empirical evidence from observations of movement speeds and limb frequencies in swimming vertebrates and flying birds and insects (Bejan & Marden 2006; Sato *et al.* 2007). However, escape and other startle responses differ from continuous swimming by being inherently unsteady and characterized by high acceleration. Moreover, millimetre-sized zooplankton performing escape jumps move from the viscous to the inertial regime during the escape (Van Duren & Videler 2003) where the drag coefficient changes dramatically as a function of the velocity. Finally, for escaping animals, natural selection may be for speed and distance rather than energy efficiency during the escape. Hydrodynamic constraints, requirements for high instantaneous force and power output, and optimization of survival rather than energy efficiency may lead to different scaling properties of jump speed from those for animals searching for food and cruising at a steady speed at high Reynolds numbers.

The energetic requirements for swimming and jumping are normally considered to constitute a small fraction of the total energy expenditure in zooplankton (Vlymen 1970; Morris *et al.* 1985, 1990; Alcaraz & Strickler 1988; Crawford 1992; Van Duren *et al.* 2003; Svetlichny & Hubareva 2005). However, the requirements for instantaneous muscle force and power production during short-lasting escape jumps may be substantial; the few indirect estimates available suggest that copepods operate at the maximum muscle power known among invertebrates and even vertebrates (see reviews in Lenz *et al.* (2004) and Askew & Marsh (2002)). While swimming in copepods is typically accomplished by the vibration of the feeding appendages, copepods jump by sequentially striking the four or five pairs of legs backwards followed by a recovery stroke where all legs are moved forward simultaneously. This 'beat cycle' may be repeated several times. Obviously, the higher the beat cycle frequency and the number of cycles in a jump, the faster and further the copepod will get, and both are critical to the success of an escape jump. The durations of both the active and the recovery phase of the jumps may be constrained by the capacity of the muscles (force) and by the requirements for high instantaneous power output, and either or both are therefore likely to determine the scaling properties of escape jumps. The maximum constant force that a muscle can output scales with its transsectional area (Hill 1950; Marden 2005), whereas in muscles that cycle (such as when moving limbs) the force output appears rather to scale with muscle mass, i.e. with organism length cubed (Marden & Allen 2002; Marden 2005). The size-scaling is less well known for aquatic organisms operating at Reynolds numbers less than 10^2, although force output has been shown to scale with body length to a power between one and three (Marden 2005).

In this study, we ask how unsteady startle velocities scale with size in small aquatic organisms that operate at intermediate Reynolds numbers, and whether the unusually high specific power outputs reported earlier for copepods are consistent with the escape speeds that one can observe. We describe the kinematics of the escape jumps in three species that vary by a factor of 10 in length (0.3–3 mm) and 10^3 in mass ($10^{-3}-1$ mg), and through direct numerical simulation we quantify the force and power that the copepod must provide to move with the observed kinematics. We then use a simple analytical model to compare the size-scaling of the kinematics and energetic properties of the escape for copepods with other organisms.

2. MATERIAL AND METHODS

2.1. Observations and experiments

Oithona davisae (adult prosome length 0.32 mm) and *Acartia tonsa* (0.75 mm) were taken from our continuous cultures whereas *Calanus finmarchicus* (3.0 mm) was collected in the Kattegat (Gulmar Fjord) and kept in the laboratory for several weeks until they were used in the experiments.

Observations were made in 1 l (*A. tonsa*, *C. finmarchicus*) or 65 ml (*O. davisae*) aquaria. We recorded escape jumps by a high-speed digital video camera, Phantom v. 4.2 Monochrome, at a resolution of 512×512 or 400×400 pixels and at frame rates between 2000 and 3500 fps. We used lenses such that the fields of view were 5×5, 15×15 or 50×50 mm^2, smallest for the smallest species. In a few cases we filmed jumps at higher magnification to describe details of limb motion. Escape jumps were either apparently spontaneous or they were provoked by tapping the side of the aquarium or approaching the copepod by a pipette tip. We analysed only the small fraction of jumps that took place in the plane perpendicular to the direction of observation. In a few cases for *C. finmarchicus*, we positioned a mirror in the diagonal of the aquarium such that we could follow the copepod in three dimensions by combining the image and the mirror image of the copepod. Illumination was provided by a 50 W halogen bulb that was pointed into the aquarium towards the camera. Experiments were conducted at 20°C (*A. tonsa* and *O. davisae*) or 12°C (*C. finmarchicus*). We analysed in total 15 jumps (including 42 jump cycles) in *A. tonsa*, 13 jumps (59 beat cycles) in *C. finmarchicus* and 24 jumps (68 beat cycles) in *O. davisae*. In addition, six jumps in *A. tonsa* and one in *O. davisae* were analysed for detailed motion of the appendages.

2.2. Kinematic description of jumps

Using ImageJ we digitized the temporal positions of the front tip and end of the prosome (the main body) and we noted the time of the start and end of the power stroke of the swimming legs. We use the terms 'beat duration' and 'pause duration' to describe the durations of the power stroke and the time interval between the termination of one and the onset of the subsequent power stroke, respectively. Thus, the pause includes the recovery stroke. The temporal positions of the body (mean of front and end of body) were used to compute velocities. In some cases we additionally digitized the positions of the tip of the urosome (tail), as well as the tips of each of either the left or the right first

antenna (if visible) and the tips of the four or five pairs of swimming legs (fifth leg is much reduced in *A. tonsa*; *O. davisae* has only four pairs of swimming legs). These were positioned relative to the animal in a coordinate system that had the tip of the head as the origin and the *z*-axis aligned with the length-direction of the body.

2.3. Direct numerical simulations

In order to estimate the force and power that the copepod has to produce to propel itself during a jump, we computed the flow field created by the copepod moving with the observed kinematics. To do so, we modelled the copepod as a prolate spheroid with major axis L equal to the prosome length and equatorial diameter to length aspect ratio, α, similar to what we measured for the three species (*O. davisae*: $\alpha = 0.51$, *A. tonsa*: $\alpha = 0.38$, and *C. finmarchicus*: $\alpha = 0.36$). For each species, the velocity variations over time, $V(t)$, of the four fastest jumps were extracted from the observations and fitted by third-order polynomials. We restricted these fits to the first power stroke in which the copepod starts from rest and only to the beat period from the beginning to the end of the power stroke. The fits were used to prescribe the motion of the spheroid in its length direction. For each of the 12 cases we solved the Navier–Stokes equation with the commercial software COMSOL. The equation was solved in the accelerated reference frame of the copepod and using cylindrical polar coordinates (r, ϕ, z) with 200 time steps of equal length. We used a no-slip boundary condition on the surface of the spheroid, which was placed at the centre of a cylindrical domain of height $30L$ and radius $15L$, assuming that on the external walls of the domain the velocity field had to satisfy $u_r = u_\phi = 0$ and $u_z = -V(t)$. All symbols used are listed in table 1.

Table 1. List of symbols.

A	constant in analytical solution
α	aspect ratio of copepod body
β	propulsion force coefficient (N m^{-2})
C_D	drag coefficient
D	drag (N)
η	dynamic viscosity (Pa s)
F	propulsion force (N)
γ	parameter in propulsion force model
K	increase of kinetic energy in beat phase (J)
L	prosome length (mm)
m	mass of copepod (kg)
m_f	mass of displaced water (kg)
ν	kinematic viscosity (m^2 s^{-1})
ϕ	azimuthal angle (rad)
P_{low}	average power at low Reynolds number (W)
P_{high}	average power at high Reynolds number (W)
Q	work to overcome drag in beat phase (J)
r	radial coordinate (mm)
R	radius of model copepod (mm)
ρ	copepod density (kg m^{-3})
ρ_f	water density (kg m^{-3})
Re	Reynolds number based on instantaneous velocity
Re_{max}	Reynolds number based on maximum velocity
Re_{mean}	Reynolds number based on average velocity
t	time (ms)
t_{max}	time when maximum velocity is reached (ms)
T	beat duration (ms)
τ	Stokes time scale (ms)
u_ϕ	azimuthal flow velocity (mm s^{-1})
u_r	radial flow velocity (mm s^{-1})
u_z	axial flow velocity (mm s^{-1})
V	copepod velocity (mm s^{-1})
V_{max}	maximum copepod velocity (mm s^{-1})
V_{mean}	average copepod velocity (mm s^{-1})
ΔV	velocity fluctuation (mm s^{-1})
W	work of propulsion force in beat phase (J)
z	axial coordinate along copepod body axis (mm)

2.4. Analytical model

We also developed a simple analytical model to facilitate interpretation of the observations. In the analytical model we approximate the copepod by a sphere with the same volume as the prolate spheroid in the direct numerical simulations. The radius of the sphere is therefore

$$R = \alpha^{2/3}\left(\frac{L}{2}\right). \tag{2.1}$$

As in the direct numerical simulations we assumed that the copepod moves linearly during the jump and we made no attempt to model the specific movements of the swimming legs that generate the propulsion force. We used the equation of motion

$$\left(m + \frac{1}{2}m_f\right)\frac{\mathrm{d}V}{\mathrm{d}t} = F - D, \tag{2.2}$$

where $m = (4/3)\pi\rho R^3$ is the mass of the copepod, $m_f = (4/3)\pi\rho_f R^3$ is the mass of the displaced water, F is the propulsion force acting on the copepod, and D is the drag. The second term on the left-hand side is due to the added mass effect. The added mass of a sphere is equal to half of the mass of the water displaced by the sphere (Lamb 1932). Copepods are slightly more dense than water, but for simplicity we assumed the copepods to be neutrally buoyant so that $\rho = \rho_f$.

The second term on the right-hand side of equation (2.2) is the hydrodynamic drag

$$D = \frac{1}{2}\pi C_D \rho_f R^2 V^2. \tag{2.3}$$

The dimensionless drag coefficient C_D depends on the Reynolds number, Re, defined as

$$Re = \frac{2RV}{\nu}, \tag{2.4}$$

where ν is the kinematic viscosity. We used the Reynolds number-dependent drag coefficient

$$C_D = \frac{24}{Re} + \frac{5}{\sqrt{Re}} + \frac{2}{5}. \tag{2.5}$$

The empirical drag expression is valid for a steadily translating sphere (Lautrup 2005; White 2006). We apply it here in a quasi-static sense. The maximum Reynolds number for escape jumps in the three copepod species ranges from 10^2 to 10^3 and we are therefore in a

Reynolds number range in which all three terms in the empirical drag coefficient (2.5) are of potential importance.

In summary we have the following equation of motion with all the terms written out explicitly:

$$2\pi\rho R^3 \frac{\mathrm{d}V}{\mathrm{d}t} = F - 6\pi\eta RV - \frac{5}{2^{3/2}}\pi\rho^{1/2}\eta^{1/2}R^{3/2}V^{3/2} - \frac{1}{5}\pi\rho R^2 V^2, \quad (2.6)$$

where $\eta = \rho_f \nu$ is the dynamic viscosity. In the equation we have neglected the history dependence of the fluid forces. The so-called Basset–Boussinesq history term is well known for the linearized Navier–Stokes equation but unknown in situations in which the advective acceleration term is of potential importance as in the present problem (Odar & Hamilton 1964). To test the applicability of equation (2.6) we made a comparison with the fluid forces obtained in direct numerical simulations of a sphere starting from rest and moving with a constant acceleration, for maximum Reynolds numbers in the range from $Re = 0.1$ to 100. This showed that equation (2.6) captures the qualitative behaviour of the fluid forces well in the whole Reynolds number range, but underestimates the magnitude of the hydrodynamic force and power by 10–20%. Therefore, we use the direct numerical simulations to determine the force and power that the copepod needs to propel, whereas we use the analytical model for our qualitative discussions.

In applying the analytical model we assume either that the copepod has a constant acceleration during the beat phase and constant deceleration during the pause phase, or that it produces a constant propulsion force in the beat phase and zero force in the pause phase. For the latter assumptions (constant propulsion force) equation (2.6) can be solved analytically if the interpolating drag term (proportional to $V^{3/2}$) is neglected. In the beat phase we find

$$V(t) = \frac{15\nu}{R}\left[A\tanh\left(\frac{At}{2\tau} + \tanh^{-1}\frac{1}{A}\right) - 1\right], \quad (2.7)$$

where we assume that the copepod starts from rest at $t = 0$, where $\tau = R^2/(3\nu)$ is the Stokes time scale (Berg 1993) and where $A = [1 + F/(45\pi\rho\nu^2)]^{1/2}$. In the coasting phase we find

$$V(t) = \frac{V_{\max}}{(1 + Re_{\max}/60)\,\mathrm{e}^{(t-t_{\max})/\tau} - Re_{\max}/60}, \quad (2.8)$$

where we assume that the coasting starts at $t = t_{\max}$ with $V = V_{\max}$ and where the Reynolds number $Re_{\max} = 2RV_{\max}/\nu$ is defined using the maximum velocity.

3. RESULTS

3.1. The jump

The sequence of events during jumps is similar between the three species (figure 1; see also the electronic supplementary material, movies S1–S3). Often a jump is initiated by the copepod reorienting by bending the urosome (tail) and folding back one or both of the first antennae. Subsequently, one pair of swimming legs after the other strikes backward at very high speed, with the posterior pair striking first and the others following, with an about 90° phase delay between legs (figure 1*b*,*c*). As a result, the copepod accelerates to its maximum velocity over a period of a few milliseconds (figure 1*a*). Subsequently, the swimming legs are recovered, all at the same time, while the

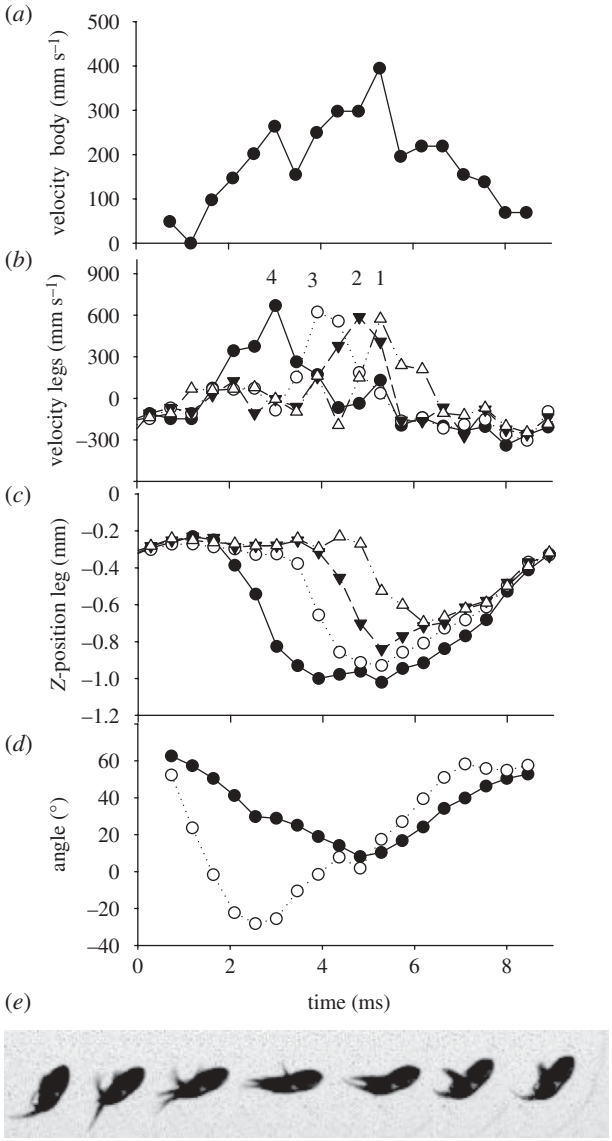

Figure 1. *Acartia tonsa*. Velocity as function of time during one beat cycle (*a*), swimming leg velocity and position relative to the body of the copepod (*b*,*c*) and orientation of the body and the tail (urosome) during a beat cycle (*d*). In (*d*) body angle is relative to the horizontal and urosome angle is relative to the body. (*e*) Shows frozen video images 3 ms apart, with the first image at time 0.7 ms, and the last image at time 8.8 ms. The copepod is viewed from the side. (*b*,*c*) Filled circle with solid line, leg 4; open circle with dotted line, leg 3; filled inverted triangle with dashed line, leg 2; open triangle with dashed-dotted line, leg 1; (*d*) filled circle with solid line, body angle; open circle with dotted line, urosome angle.

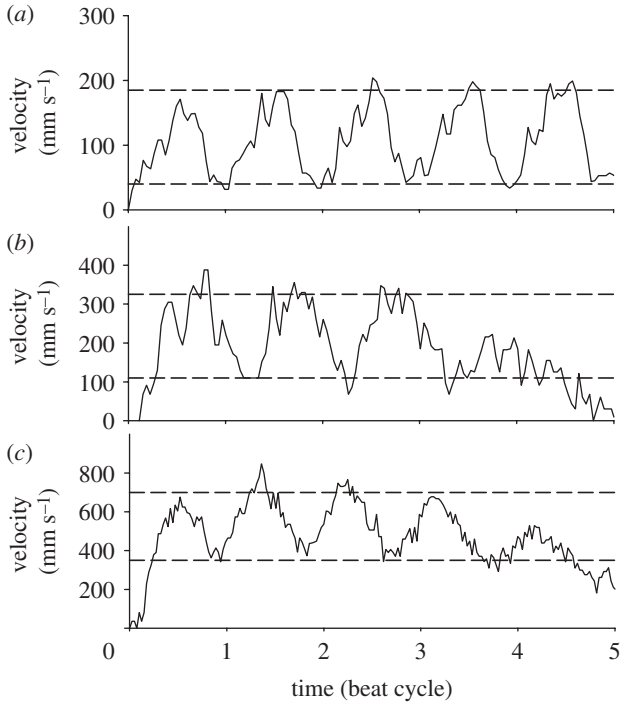

Figure 2. Velocity fluctuations during a series of beat cycles in three species of copepods. The time has been normalized by the average duration of a beat cycle (table 2). The dotted lines (eye-fitted) show the maximum and minimum velocities that were used to estimate ΔV. Velocities were averaged over 0.5 ms intervals. (*a*) *O. davisae*, $\Delta V/V_{\mathrm{mean}} = 0.6$; (*b*) *A. tonsa*, $\Delta V/V_{\mathrm{mean}} = 0.5$; (*c*) *C. finmarchicus*, $\Delta V/V_{\mathrm{mean}} = 0.3$.

animal coasts forward at a decelerating velocity. If it is the last beat cycle in a jump, the antennae unfold and the copepod eventually stops. Otherwise, the sequence is repeated after a delay. A jump may consist of one or many consecutive beat cycles (we observed up to nine) and the velocity of the copepod fluctuates accordingly (figure 2).

The animal appears to use the urosome to steer, but the steering mechanism seems more like a 'contra oar' than a rudder. Because the swimming legs are all on the ventral side of the animal, their beating would tend to rotate the animal along its length axis and around its side–side axis (pitch); the urosome compensates for that. For the example shown in figure 1 and in the electronic supplementary material, movie S1, the animal starts the jump in an almost vertical position. As the first pair of legs strikes, the urosome is bent backward (dorsally) and the animal turns such that its jump direction becomes horizontal (ventral side up). As the subsequent leg-pairs strike, the urosome is being bent more and more forward (ventrally), apparently preventing the rotation of the animal. At the end of the beat cycle, as the animal decelerates, the urosome is turned the most forward (ventrally), and the animal swings into a vertical position again. This is repeated during all four consecutive beat cycles in this particular animal, but the exact steering may vary substantially between jumps and the copepod seems to have full control over the direction of the jump.

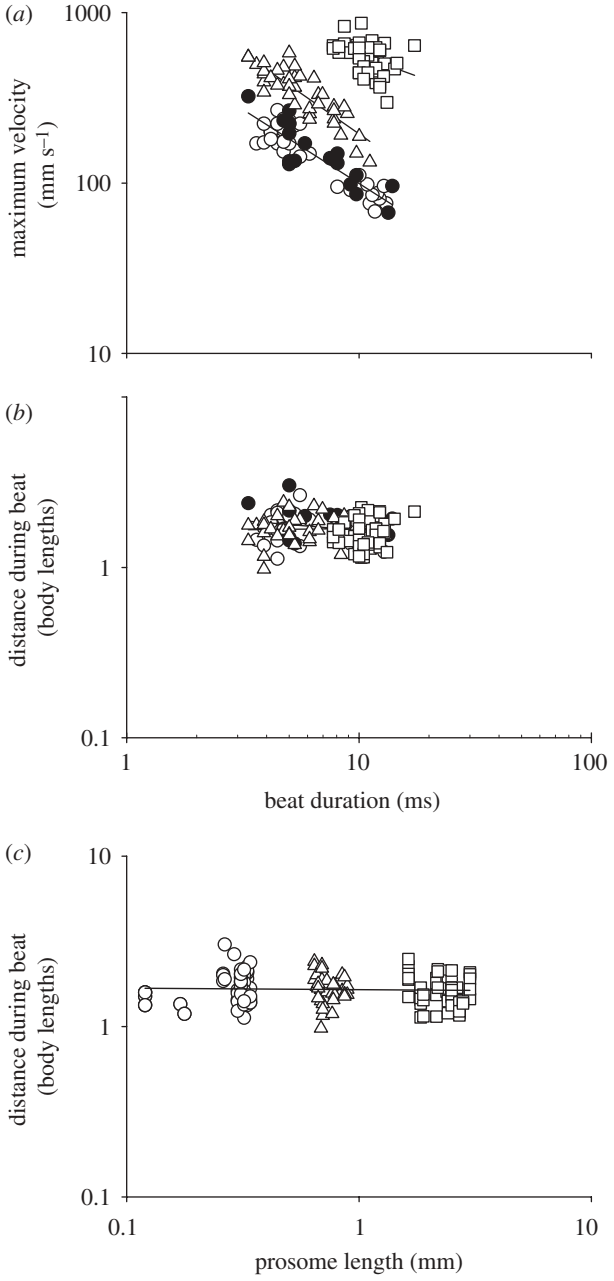

Figure 3. (*a*) Maximum velocity during a jump as a function of the duration of the power stroke and (*b*) the specific distanced covered during the power stroke as a function of the duration of the power stroke or (*c*) size of the copepod for three species of copepods. The slopes of the power-law regressions in panel (*a*) are −0.9, −1.0 and −0.5 for *O. davisae*, *A. tonsa* and *C. finmarchicus*, respectively, and they were all significantly different from zero ($p < 0.01$). The regression line in (*c*) is not statistically significant. Open circle, *O. davisae* with eggs; filled circle, *O. davisae* without eggs; open triangle, *A. tonsa*; open square, *C. finmarchicus*.

3.2. Beat duration

The duration of the power stroke of the swimming legs varies substantially between the jumps, and the maximum velocity during a beat decreases with the duration of the beat (figure 3*a*). In the two smaller species, velocity varies almost inversely with beat duration; in the larger species the dependency is less pronounced. *Oithona davisae* is an ambush feeder that

Table 2. Characteristics of experimental animals (only adults and late copepodites) and their escape jumps. In *O. davisae* and *A. tonsa*, only escape jumps are included, while repositioning jumps are not. One-way ANOVAs revealed that differences between species were statistically significant at $p < 0.05$ or less for all comparisons, except for 'specific distance per beat' and 'Strouhal number'.

	body size (adults) (mm)	max speed (mm s^{-1})	average speed (mm s^{-1})	beat duration (ms)	pause duration (ms)	distance per beat cycle		distance per beat		beat cycle frequency (Hz)	Strouhal number	ratio pause/ beat duration
						absolute (mm)	specific body length	absolute (mm)	specific body length			
Oithona (escapes)	0.3	198 ± 42	101 ± 21	4.8 ± 1.0	2.6 ± 1.1	0.75 ± 0.16	2.16 ± 0.56	0.58 ± 0.12	1.71 ± 0.4	137 ± 12	0.24 ± 0.06	0.63 ± 0.19
Acartia (escapes)	0.74 ± 0.08	378 ± 96	241 ± 53	4.4 ± 0.7	3.2 ± 0.7	1.85 ± 0.24	2.63 ± 0.38	1.20 ± 0.20	1.71 ± 0.32	134 ± 20	0.23 ± 0.04	0.71 ± 0.19
Calanus	2.35 ± 0.38	634 ± 132	333 ± 96	10.8 ± 1.9	9.4 ± 4.0	7.96 ± 8.12	3.53 ± 3.7	3.73 ± 0.92	1.64 ± 0.31	53 ± 12	0.23 ± 0.06	0.87 ± 0.31

most of the time hangs motionless in the water, only interrupted by occasional repositioning jumps. The segregation of jumps into slow and fast ones corresponds to repositioning and escape jumps (figure 3*a*). *Acartia tonsa* switches between ambush feeding and feeding while swimming and here again the longer beat durations correspond to reposition jumps during ambush feeding. For later analyses, we separated escape from repositioning jumps at a set beat duration (7 ms for both species). All jumps in *C. finmarchicus* are escape jumps, albeit of variable strengths. In *O. davisae*, those females that carry eggs jump slightly slower than those that do not, but the difference is not statistically significant (analysis of residuals; $p > 0.05$).

If only escape jumps are considered, the average beat duration is similar among the two smaller species, but lasts about twice as long in the larger species (table 2). Irrespective of the duration of the stroke phase, the distance covered during the stroke is almost constant and averages a little less than two body lengths in all species (figure 3*b*,*c* and table 2).

3.3. Pause duration and beat cycle frequency

The duration of the pause following a power stroke is independent of the duration of the stroke (within species), except in *C. finmarchicus*, where the two are positively correlated ($R = 0.55$, $p < 0.05$). Average pause durations are similar among the two smaller species but pauses last about three times longer in the larger species, whether considering only escape jumps (table 2) or all jumps (data not shown). Accordingly, the resulting beat cycle frequency, (stroke duration + pause duration)$^{-1}$, varies between the two smaller species and the larger one by a factor of 2.5 (table 2). The Strouhal number, i.e. the beat cycle frequency times the stroke amplitude (assumed to be one body length) divided by the average escape velocity, is remarkably constant between species averaging 0.23–0.24 (table 2).

The ratio of pause to stroke duration varies significantly between the three species and increases with the size of the copepods (figure 4*a* and table 2). That is, larger copepods have relatively longer pauses between strokes. The copepod keeps gliding forward during the pause due to inertia, most pronounced for the large species (see below). Because both coasting distance and relative pause duration increase with size, the distance covered during the entire beat cycle (stroke + pause) increases with size (figure 4*b*). The velocity averaged over the entire beat cycle decreases with increasing pause duration, which is most obvious when comparing across species and only statistically significant within species for *A. tonsa* (figure 4*c*).

3.4. Maximum velocity

The maximum velocity during the beat cycle increases with copepod size (table 2). Our data are consistent with those from the literature, but expand the range to smaller sizes and together with literature data suggest a power-law dependency with an exponent of 0.65 (figure 5). The size-scaling of escape velocities is

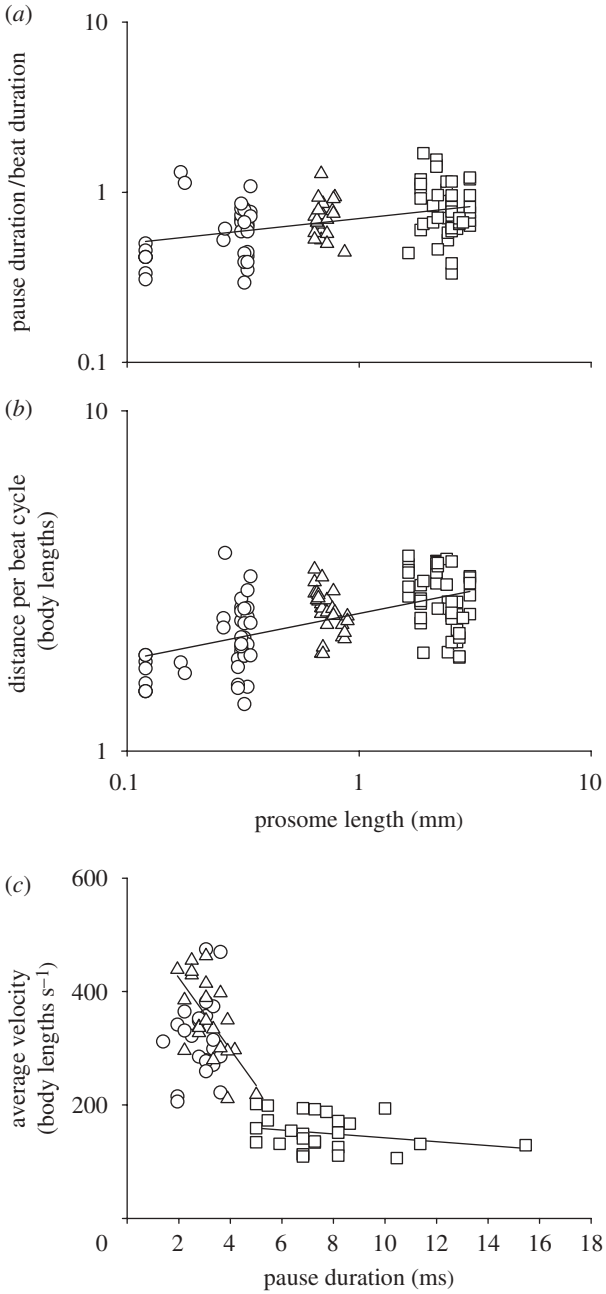

Figure 4. (*a*) Ratio of pause to beat duration (escape jumps only) as a function of copepod size, (*b*) specific distance covered per beat cycle as a function of copepod size and (*c*) average specific velocity as a function of pause duration in three species of copepods. In (*c*) only jumps with beat durations less than 6 ms (*A. tonsa* and O. *davisae*) or 11 ms (*C. finmarchicus*) have been included. The lines shown in the panels are regression lines: (*a*) slope = 0.15; $p < 0.0005$; (*b*) slope = 0.14; $p < 0.0005$. Open circle, *O. davisae*; open triangle, *A. tonsa*; open square, *C. finmarchicus*.

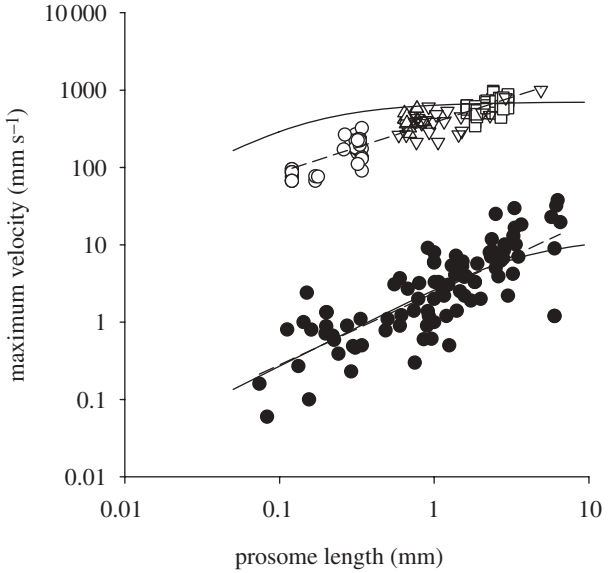

Figure 5. Escape and cruise velocities of pelagic copepods as measured in this study and reported in the literature. The dashed lines are power laws fitted to the data, which yield powers of 0.65 and 0.93 for the escape and cruise velocities, respectively. The solid lines are velocities predicted from equation (4.3), either by fitting the expression to the data (cruise velocities, with the propulsion force, F, as the free variable to be estimated), or by computing velocities using an estimate of the coefficient β from the data in figure 8. We used the definition $\beta = F/(\pi R^2)$ and found the average $101 \pm 40\ \mathrm{N\ m^{-2}}$ ($\pm$s.d.; $n = 12$), with R taken as $\frac{1}{2} \times 0.42 \times$ length of the copepod from the average aspect ratio of copepods in this study. The literature observations on cruise velocities were taken from the data compilations of Máuchline (1998) and Kiørboe & Bagøien (2005) supplemented with data from Titelman (2003) and Goetze & Kiørboe (2008) as well as own unpublished observations on *Acartia grani*. Adult males were excluded from the compilation. Literature jump velocities were from Yen & Strickler (1996), Buskey *et al.* (2002), Waggett & Buskey (2007, 2008), Burdick *et al.* (2007) and Kiørboe *et al.* (2009). Regression equations for escape and cruise velocities (v, $\mathrm{mm\ s^{-1}}$) as functions of prosome length (L, mm) are: $\log v_{\mathrm{escape}} = 2.58 + 0.65 \log L$, $r^2 = 0.85$; $\log v_{\mathrm{cruise}} = 0.38 + 0.93 \log L$. Open circle, *Oithona*; open triangle, *Acartia*; open square, *Calanus*; open inverted triangle, literature, escape; filled circle, literature, cruise.

significantly different from the size-scaling of cruising copepods, where velocity increases almost proportionally to copepod size (figure 5).

3.5. Force and power

We fitted the analytical model, equation (2.7), to the observed temporal variation in velocity during the beat phase and predicted the subsequent pause phase from equation (2.8) in typical examples for the three species (figure 6). Both the acceleration and the coasting are captured well by the analytical model. We use the observed kinematics and direct numerical simulations to obtain the temporal force variation (figure 7) and estimates of the average specific force and power (figure 8). The time dependence of the force is similar for all species with an initial increase to a near constant level, and a decline at the end of the power stroke. The average force has been expressed relative to either the body weight or the cross-sectional area of the copepod (πR^2) and is equally (in)consistent with either scaling (figure 8). The weight- and area-specific force outputs vary between 90–$330\ \mathrm{N\ kg^{-1}}$ and 50–$150\ \mathrm{N\ m^{-2}}$, respectively, between the three species, with *A. tonsa* being the most forceful. The average specific power output also showed no clear trends

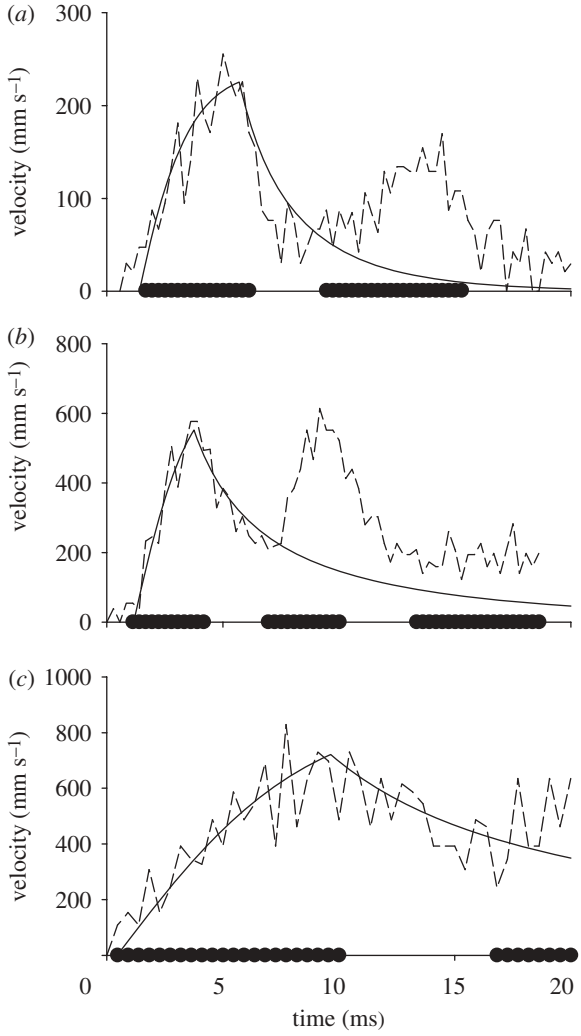

Figure 6. Observed velocity variations during typical escape jumps of (*a*) *O. davisae*, (*b*) *A. tonsa* and (*c*) *C. finmarchicus* and fits of the analytical model during the beat phase (equation (2.7)) and prediction of the model during coasting in the pause phase (equation (2.8)). In fitting the analytical model, the only free variable (force, F) was estimated (dashed line, observed; solid line, fitted/predicted; filled circle, beat phase).

among species (figure 8) and it varied somewhat between species, lowest in *C. finmarchicus* (average 30 W (kg body mass)$^{-1}$), highest in *A. tonsa* (100 W kg^{-1}) and intermediate in *O. davisae* (40 W kg^{-1}).

4. DISCUSSION

4.1. Force production and power output

Startle responses in zooplankton and other organisms attempting to escape a predator are likely to be executed with the maximum muscular force and power output that the organism can produce. We have estimated these parameters from observed velocity variation during the course of copepod escape jumps by means of direct numerical simulations. Our method represents an advance over previous attempts (Vlymen 1970; Fields 2000) since we solve the Navier–Stokes equation directly and thus include the

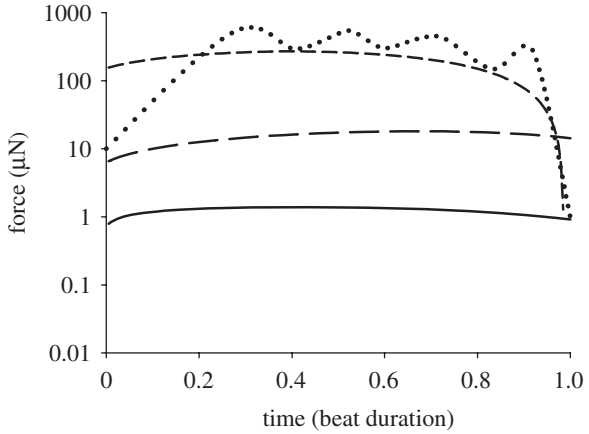

Figure 7. Temporal variation in propulsion force during the beat phase computed for three example jumps by the direct numerical simulation. Shown also are direct measurements of forces working on an adult male *C. finmarchicus* during a power stroke (from Lenz *et al.* (2004), their fig. 2). The time has been normalized by the beat duration of the jumps (solid line, *O. davisae*; long dashed line, *A. tonsa*; dashed line, *C. finmarchicus*; dotted line, Lenz *et al.* (2004)).

so-called history term. Our approach, however, ignores the motion of the swimming legs and the estimated parameters are, thus, preliminary and, presumably, conservative. We nevertheless have confidence in our estimates, because the estimate of forces compare well with—but are slightly smaller than—those measured experimentally in similar-sized copepods tethered to a force transducer (Lenz & Hartline 1999; Lenz *et al.* 2004) or a spring (Alcaraz & Strickler 1988). Specifically, the observations of Lenz *et al.* (2004) on *C. finmarchicus* compare favourably with our estimates for the same species, both in terms of magnitude and temporal variation during the beat phase (figure 7). The discrepancy in magnitude may simply reflect the fact that escape intensity varies between escape events (figure 3*a*), e.g. as a function of the stimulus (Waggett & Buskey 2007), and the escape velocities recorded by Lenz *et al.* (2004) were higher than those recorded in our experiments.

Hill (1950) argued that the maximum force that a muscle can produce scales with its cross-sectional area whereas Marden (2005) maintained alternatively that muscle-motor performance in muscles of 'larger' organisms that cycle at a steady rate should scale with muscle mass. Our data are somewhere in between, although it is questionable to deduce a proper scaling for just three species, where species-specific and temperature differences may become important. Nevertheless, we may compare the force magnitudes found here with those reported in the literature. Marden (2005) examined how the maximum net force production of isolated muscles during maximum tension as well as that of intact organisms (with muscles attached to the lever system of the animal limbs) vary as a function of muscle mass (figure 8*b*). The mass-specific maximum net force output is strikingly constant among larger (Re more than 100) intact organisms, including both vertebrates and invertebrates, averaging a temperature independent value of 57 N(kg muscle)$^{-1}$. The

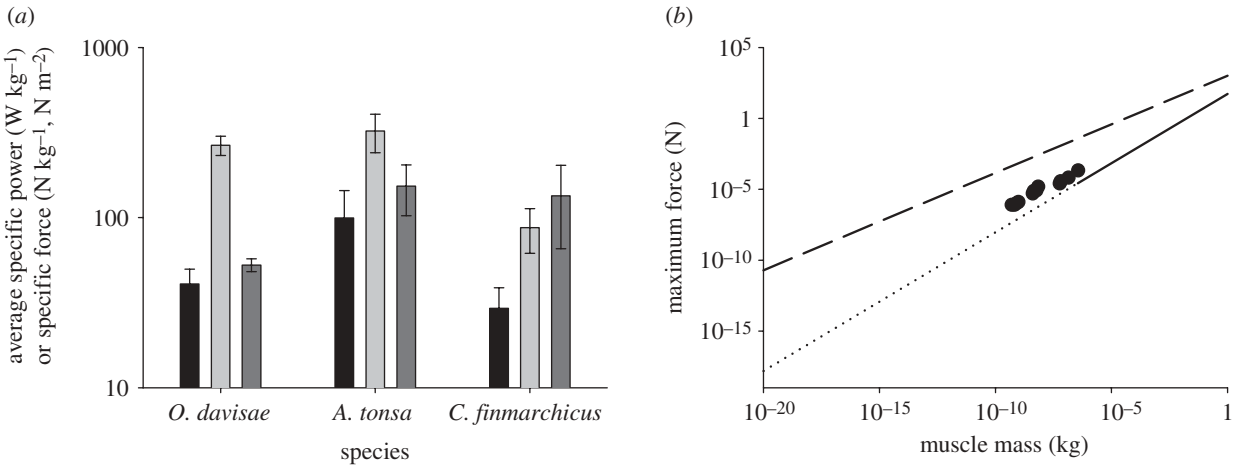

Figure 8. (*a*) Average (±s.d.) specific power and force output in three species of jumping copepods estimated using the simulation model and observed jump kinematics. Data have been averaged for the four most powerful jumps of each species. Power production has been normalized with body mass, and propulsion force has been normalized with either body mass or with the cross-sectional area of the copepod (πR^2). One-way ANOVA with Tukey *post hoc* tests show that only the mass-specific forces differ between species, with *C. finmarchicus* being significantly different from the two other species (solid black bar, body mass-specific power; light grey bar, body mass-specific force; dark grey bar, area-specific force). (*b*) Relation between force production of individual muscles (group 1) or of flying, swimming, and running animals (group 2) and muscle mass as reported by Marden (2005). Our data for jumping copepods are included in this plot (dashed line, group 1 motors; solid line, group 2 motors; dotted line, group 2, extrapolated; filled circles, jumping copepods).

corresponding values for our three copepod species, integrated over the entire beat cycle, averaged 100–300 N (kg body)$^{-1}$, or 500–1500 N (kg muscle)$^{-1}$ if the jump-muscle mass is 20 per cent of the body mass (cf. Lenz *et al.* 2004). Thus, the maximum specific force output of copepod jump muscles is more than an order of magnitude higher than that recorded in larger animals translating at a steady pace, even where the copepods overlap in size with the motors examined by Marden (2005), but well below that maximally produced by individual muscles (figure 8*b*). While copepods are suspected to be able to store mechanical energy in elastin (Alcaraz & Strickler 1988), this capacity cannot explain the high force output because our estimate is averaged over an entire beat cycle (i.e. including the pause). Marden (2005) suggested that the constancy of the mass-specific net force production found among animal and mechanical motors alike is related to the longevity of the motor system, which varies inversely with performance and appears to decline rapidly at loads greater than 100 N kg^{-1}. The short intense burst of an escape motor would not be similarly constrained. Even though the legs are referred to as *swimming* legs, they are, however, in most copepods only used for jumps. The musculatures of the legs are similar among taxonomically diverse copepods (Boxshall 1992), but it is difficult to figure out the exact lever system from existing descriptions of the muscle arrangements because the muscles do not attach to the leg itself and the power stroke is produced indirectly (Boxshall 1985). While the force produced by isolated muscles of copepods cannot exceed that suggested in figure 8*b* (group 1), the high force production in escaping copepods would suggest a lever system specifically adapted for startle responses and with a gearing different from the lever system of appendages used for continuous translation. This may explain why the startle responses of copepods are an order of magnitude higher than those recorded in most other similarly sized aquatic animals (Lenz *et al.* 2004) that use the same propulsion apparatus for escape and steady translation. It is striking that shrimps, which also have separate propulsion systems for escape and swimming, have escape velocities similar to copepods and higher than those of all others in the data compilation of Lenz *et al.* (2004).

The estimated power output during escapes is similarly impressive and compares rather well with previous, independent estimates for copepods. Thus, from observations of the kinematics of limb movements and measurement of the forces working on the swimming legs of a tethered copepod Lenz *et al.* (2004) estimated 60 W kg^{-1} for *C. finmarchicus* integrated over the entire beat cycle, 2–4 times our average for this species, but similar to our overall average estimate for the three species. Estimates for other species, arrived at in similar ways, are of similar order of magnitude (Svetlichnyy 1987; Lenz & Hartline 1999). If the muscles used for propulsion account for 20 per cent of the body mass then the power output is approximately 300 W (kg muscle)$^{-1}$ and the escaping copepods outpower most other invertebrates and produce as much power as the most powerful vertebrate muscles (Askew & Marsh 2002).

4.2. The cost of a fluctuating translation velocity

Most escape jumps consist of consecutive beat cycles and are characterized by a highly fluctuating velocity of the copepod (figure 2). The fluctuating velocity has an energetic cost as compared with a steady motion. To estimate the cost of the velocity fluctuation on the average power output, we draw on a simple model developed by Alexander (2003) for other swimmers

with alternating beats and pauses. Let V_{mean} be the average speed and ΔV the amplitude of the speed variation (figure 2) and assume that the copepod during the beat phase moves with constant acceleration from the minimum speed $V_{\mathrm{mean}} - \Delta V$ to the maximum speed $V_{\mathrm{mean}} + \Delta V$ and that it during the pause phase moves with constant deceleration from $V_{\mathrm{mean}} + \Delta V$ to $V_{\mathrm{mean}} - \Delta V$. With these assumptions made in the copepod model we find from integrating the force, F, over time in equation (2.2) that the average power of the propulsion force at low Reynolds number, i.e. with only the first term in equation (2.5), is

$$P_{\mathrm{low}} = 6\pi\eta R\, V_{\mathrm{mean}}^2 \left[1 + \frac{1}{3}\left(\frac{\Delta V}{V_{\mathrm{mean}}}\right)^2\right], \tag{4.1}$$

and that the average power of the propulsion force at high Reynolds number, i.e. with only the third term in equation (2.5), is

$$P_{\mathrm{high}} = \frac{1}{5}\pi\rho R^2\, V_{\mathrm{mean}}^3 \left[1 + \left(\frac{\Delta V}{V_{\mathrm{mean}}}\right)^2\right]. \tag{4.2}$$

Equation (4.2) is identical to the result derived by Alexander (2003) who considered the high Reynolds number case and more specifically modelled the water beetle studied experimentally by Nachtigall (1960, 1980). Equations (4.1) and (4.2) indicate that the work done against drag on the copepod increases due to the speed variation and that the correction terms are proportional to the relative speed variation squared irrespective of the Reynolds number. The equations therefore suggest that, in order to minimize the energy expenditure to escape with a given average speed V_{mean} the copepod should minimize the amplitude of the swimming speed variation ΔV and hence the pause duration as much as possible within the anatomical constraints of the propulsion apparatus. However, the increase in average power due to the speed variation is fairly small since the correction terms depend on the relative speed variation squared. For *C. finmarchicus* $\Delta V/V_{\mathrm{mean}} \approx 0.3$ (figure 2*c*), and the increase in energy expenditure is about 10 per cent from equation (4.2); for the smaller *O. davisae*, $\Delta V/V_{\mathrm{mean}} \approx 0.6$ (figure 2*a*), but the increase in energy expenditure is also only about 10 per cent, because here the low Reynolds number expression in equation (4.1) is the better approximation. The fluctuations therefore do not have a dramatic effect on the average power expenditure.

4.3. Scaling of escape speed

Equation (2.2) shows that when the copepod accelerates, it ultimately reaches a maximum velocity when the drag compensates the propelling force: $F = D$. If the maximum propulsion force that the copepod can produce is proportional to its length squared as our data and some theories suggest, it follows that V_{max} is proportional to R at low Reynolds number where $C_D \approx 24/Re$, and size-independent at high Reynolds number where C_D tends to a constant value of 2/5. At intermediate Reynolds number the scaling becomes somewhere in between. With this formulation, the dependence of the translation velocity is strictly speaking not a power law. Ignoring the square root term in the drag coefficient (2.5) and assuming $F = D$ we find

$$V_{\mathrm{max}} = \frac{15\nu}{R}\left[\sqrt{1 + \frac{\beta R^2}{45\,\rho\,\nu^2}} - 1\right], \tag{4.3}$$

where we assume the scaling $F = \beta\pi R^2$. This expression can be fitted to the observed cruise velocities and yields a nice fit with near proportionality between speed and size (figure 5). We can also predict what the steady-state escape velocity should be using the estimate $\beta = 101 \pm 40\ \mathrm{N\ m^{-2}}$ from the data in figure 8, but the expected near size-independency for escaping copepods is inconsistent with observations. The reason is that equation (4.3) assumes steady state but the jumping copepod never reaches terminal velocity before the end of the power stroke—it is of too short a duration—and the 'unexpected' scaling is a result of the unsteady motion. This implies that the scaling of the maximum jump speed is instead governed by the duration of the active stroke phase The high force and power output estimated above and the need for speed in an escaping copepod would argue that limb motion and escape speeds are ultimately limited by the force and power output that can be produced, and therefore that beat duration is as short as the maximum force output allows. The size-scaling of startle response speeds in fishes and other aquatic organisms in the size range 2–500 mm similarly deviates from predictions of classical models and although the velocities are much slower they scale with size the same way as in the copepods, i.e. with length to a power of 0.65 (Lenz *et al.* 2004).

4.4. Distance covered during a power stroke

Because the distance covered during the active phase is approximately two body lengths for all three species and independent of the beat duration T (figure 3*b*), it follows that the maximum speed in a jump starting from rest is approximately $V = 4L/T$, and that V scales approximately inversely with T as observed (figure 3*a*). We can rationalize this observation by noting that the body and the legs experience similar drag since the cross-sectional area of a pair of striking swimming legs is similar to the cross-sectional area of the translating copepod (Morris *et al.* 1990; Lenz *et al.* 2004) and the speed through the water of the striking swimming legs is similar to the translation speed of the copepod (figure 1). If $C_D \sim Re^{-\gamma}$ with $\gamma = 1$ at low Reynolds number and $\gamma = 0$ at high Reynolds number, we find that the propulsion force is proportional to $T^{-(2-\gamma)}$ and that the drag on the body is proportional to $V^{2-\gamma}$. Balance of the two force terms then leads to $V \sim T^{-1}$ as observed.

4.5. Pause duration and beat cycle frequency

In a jump consisting of a series of beat cycles, the duration of the pause between power strokes may be equally important as the acceleration and maximum

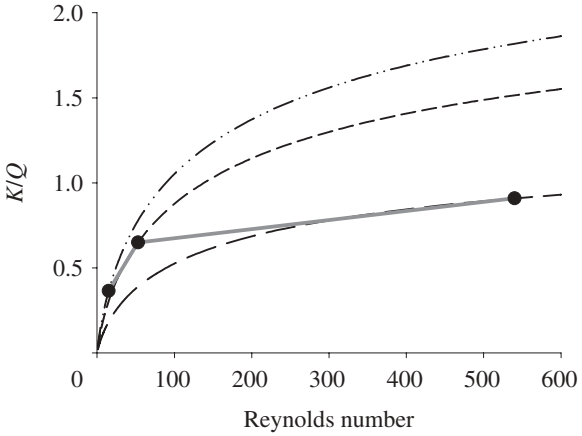

Figure 9. The ratio K/Q of work done to accelerate the copepod and the added mass during the beat phase to the work done to overcome drag in the beat phase as a function of the Reynolds number for various values of the relative velocity fluctuations $\Delta V/V_{\mathrm{mean}}$ as shown in equation (4.6). The Reynolds number is here computed for the average velocity. The dots are corresponding values of Reynolds number and $\Delta V/V_{\mathrm{mean}}$ typical of the three copepod species (figure 2): *O. davisae* ($Re_{\mathrm{mean}} = 15$; $\Delta V/V_{\mathrm{mean}} = 0.6$ (dashed-dotted line)), *A. tonsa* ($Re_{\mathrm{mean}} = 53$; $\Delta V/V_{\mathrm{mean}} = 0.5$ (short-dashed line)), and *C. finmarchicus* ($Re_{\mathrm{mean}} = 540$; $\Delta V/V_{\mathrm{mean}} = 0.3$ (long-dashed line)). These values have been connected by a grey line. The K/Q ratio is an estimate of the ratio of pause to beat duration, and increases with the Reynolds number, also when taking into account the variation in $\Delta V/V_{\mathrm{mean}}$.

velocity in determining the escape success. We observed that the relative pause duration increases with size (figure 4*a* and table 2). This actually follows from the fluctuating character of the escape velocity and the Reynolds number dependence of the hydrodynamic force, as can be demonstrated from our analytical model. If the duration of the beat phase is always $T = 4R/V_{\mathrm{mean}}$ then, from equation (2.2), the total work done by the propulsion force during the beat phase is the sum of the increase of the kinetic energy of the copepod and the added mass, K, and the work done against drag on the copepod, Q. If we neglect the correction terms due to the velocity fluctuations in the calculation of Q (cf. above), we find

$$K = 4\,\pi\rho R^3\, V_{\mathrm{mean}}\,\Delta V \tag{4.4}$$

and

$$Q = 2\,\pi C_D\,\rho R^3\, V_{\mathrm{mean}}^2. \tag{4.5}$$

The ratio of the two work terms is therefore

$$\frac{K}{Q} = \frac{2\Delta V/V_{\mathrm{mean}}}{C_D} = \frac{10Re_{\mathrm{mean}}\Delta V/V_{\mathrm{mean}}}{120 + 25\sqrt{Re_{\mathrm{mean}}} + 2Re_{\mathrm{mean}}} \tag{4.6}$$

which depends on the Reynolds number $Re_{\mathrm{mean}} = 2RV_{\mathrm{mean}}/\nu$. The work done to increase the kinetic energy in the beat phase is used to overcome the drag on the coasting copepod in the pause phase. The ratio K/Q is therefore equal to the ratio of the work done to overcome drag on the copepod in the pause phase and in the beat phase, respectively. If we as above assume that the coasting takes place with constant deceleration, it follows that the ratio between the duration of the pause phase and the duration of the beat phase is equal to the ratio K/Q. Equation (4.6) predicts that this ratio increases with increasing Reynolds number in agreement with our observations, even when considering the decreasing ratio of $\Delta V/V_{\mathrm{mean}}$ with increasing size and Reynolds number (figures 2 and 9). This result is not specific to the escaping copepods but applies generally to swimmers with alternating power strokes and pauses.

The sum of the beat and pause duration determines the beat cycle frequency. The product of the beat cycle frequency and the beat amplitude divided by the average velocity is the Strouhal number. It is well documented that the propulsion efficiency is highest at Strouhal numbers between 0.2 and 0.4 (Anderson *et al.* 1998) and many flying and swimming organisms operate within this range (Taylor *et al.* 2003). The Strouhal number for the escaping copepods is similar among the three species examined here and within the range where the propulsion efficiency is highest (table 2), thus suggesting optimal design of the swimming legs and the body shape for escape responses.

5. CONCLUSION

Startle responses in copepods and other organisms are characterized by high accelerations, fluctuating speeds and short durations. Because of this unsteady nature, the size-scaling of startle velocities are different from the size-scaling of cruise velocities in steadily translating organisms. In small aquatic organisms, where the hydrodynamics is Reynolds number dependent, the scaling may be further modified. Startle responses are also constrained differently from swimming velocities; in cruising (Bejan & Marden 2005) and migrating (Hedenström 2003) animals, energy efficiency is crucial and governs the size-scaling. Startle responses, in contrast, are limited by the maximum short-term force and power output that the organism can produce. Pelagic copepods appear to be designed for optimal propulsion efficiency during escape jumps and the arrangement of their musculature probably tuned for an unusual performance, making them particularly efficient in escaping predators and accounting for their evolutionary success in the ocean.

This work was supported by grants from the Danish Council for Independent Research and the Niels Bohr foundation.

REFERENCES

Alcaraz, M. & Strickler, J. R. 1988 Locomotion in copepods: pattern of movements and energetics of *Cyclops*. *Hydrobiologia* **167/168**, 409–414. (doi:10.1007/BF00026333)

Alexander, R. McN. 2003 *Principles of animal locomotion*. Princeton, NJ: Princeton University Press.

Anderson, J. M., Streitlien, K., Barrett, D. S. & Triantafyllou, M. S. 1998 Oscillating foils of high propulsive efficiency. *J. Fluid Mech.* **360**, 41–72. (doi:10.1017/S0022112097008392)

Askew, G. N. & Marsh, R. L. 2002 Muscle design for maximum short-term power output: quail flight muscle. *J. Exp. Biol.* **205**, 2153–2160.

Berg, H. C. 1993 *Random walks in biology*, expanded edn. Princeton, NJ: Princeton University Press.

Bejan, A. & Marden, J. H. 2006 Unifying constructal theory for scale effects in running, swimming and flying. *J. Exp. Biol.* **209**, 238–248. (doi:10.1242/jeb.01974)

Biewener, A. A. 2003 *Animal locomotion.* Oxford, UK: Oxford University Press.

Boxshall, G. A. 1985 The comparative anatomy of two copepods, a predatory calanoid and a particle-feeding mormonilloid. *Phil. Trans. R. Soc. Lond. B* **311**, 303–377. (doi:10.1098/rstb.1985.0155)

Boxshall, G. A. 1992 Copepoda. *Microsc. Anat. Invert.* **9**, 347–384.

Burdick, D. S., Hartline, D. K. & Lenz, P. H. 2007 Escape strategies in co-occurring calanoid copepods. *Limnol. Oceanogr.* **52**, 2373–2385.

Buskey, E. J., Lenz, P. H. & Hartline, D. K. 2002 Escape behaviour of planktonic copepods in response to hydrodynamic disturbances: high speed video analysis. *Mar. Ecol. Prog. Ser.* **235**, 135–146. (doi:10.3354/meps235135)

Crawford, D. W. 1992 Metabolic cost of motility in planktonic protists: theoretical considerations on size scaling and swimming speed. *Microb. Ecol.* **24**, 1–10. (doi:10.1007/BF00171966)

Fields, D. M. 2000 Characteristics of the high frequency escape reactions of *Oithona* sp. *Mar. Fresh. Behav. Physiol.* **34**, 21–35. (doi:10.1080/10236240009379057)

Goetze, E. & Kiørboe, T. 2008 Heterospecific mating and species recognition in the planktonic marine copepods *Temora stylifera* and *T. longicornis*. *Mar. Ecol. Prog. Ser.* **370**, 185–198. (doi:10.3354/meps00076)

Hedenström, A. 2003 Scaling migration speed in animals that run, swim and fly. *J. Zool.* **259**, 155–160. (doi:10.1017/S0952836902003096)

Hill, A. V. 1950 The dimensions of animals and their muscular dynamics. *Sci. Progr.* **38**, 209–230. (doi:10.1038/164820b0)

Humes, A. G. 1994 How many copepods? *Hydrobiologia* **292/293**, 1–7. (doi:10.1007/BF00229916)

Kiørboe, T. & Bagøien, E. 2005 Motility patterns and mate encounter rates in planktonic copepods. *Limnol. Oceanogr.* **50**, 1999–2007.

Kiørboe, T., Andersen, A., Langlois, V. J., Jakobsen, H. H. & Bohr, T. 2009 Mechanisms and feasibility of prey capture in ambush feeding zooplankton. *Proc. Natl Acad. Sci. USA* **106**, 12 394–12 399. (doi:10.1073/pnas.0903350106)

Lamb, H. 1932 *Hydrodynamics*, 6th edn. New York, NY: Dover Publications.

Lautrup, B. 2005 *Physics of continuous matter.* Bristol, UK: Institute of Physics Publishing.

Lenz, P. H. & Hartline, D. K. 1999 Reaction times and force production during escape behavior of a calanoid copepod, *Undinula vulgaris*. *Mar. Biol.* **133**, 249–258. (doi:10.1007/s002270050464)

Lenz, P. H., Hower, A. E. & Hartline, D. K. 2004 Force production during pereiopod power strokes in *Calanus finmarchicus*. *J. Mar. Syst.* **49**, 133–144. (doi:10.1016/j.jmarsys.2003.05.006)

Marden, J. H. 2005 Scaling of maximum net force output by motors used for locomotion. *J. Exp. Biol.* **208**, 1653–1664. (doi:10.1242/jeb.01483)

Marden, J. H. & Allen, L. R. 2002 Molecules, muscles, and machines: universal performance characteristics of motors. *Proc. Natl Acad. Sci. USA* **99**, 4162–4166. (doi:10.1073/pnas.022052899)

Máuchline, J. 1998 The biology of calanoid copepods. *Adv. Mar. Biol.* **33**, 1–710.

Morris, M. J., Gust, G. & Torres, J. J. 1985 Propulsion efficiency and cost of transport for copepods: a hydromechanical model of crustacean swimming. *Mar. Biol.* **86**, 283–295. (doi:10.1007/BF00397515)

Morris, M. J., Kohlhage, K. & Gust, G. 1990 Mechanics and energetics of swimming in the small copepod *Acanthocyclops robustus* (Cyclopoida). *Mar. Biol.* **107**, 83–91. (doi:10.1007/BF01313245)

Nachtigall, W. 1960 Über Kinematik, Dynamik und Energetik des Schwimmens einheimischer Dytisciden. *Zeitschrift für Vergleichende Physiologie* **43**, 48–118.

Nachtigall, W. 1980 Mechanics of swimming in water-beetles. In *Aspects of animal movement* (eds H. Y. Elder & E. R. Trueman), pp. 107–124. Cambridge, UK: Cambridge University Press.

Odar, F. & Hamilton, W. S. 1964 Forces on a sphere accelerating in a viscous fluid. *J. Fluid Mech.* **18**, 302–314. (doi:10.1017/S0022112064000210)

Sato, K. *et al.* 2007 Stroke frequency, but not swimming speed, is related to body size in free-ranging seabirds, pinnipeds and cetaceans. *Proc. R. Soc. Lond. B* **274**, 471–477. (doi:10.1098/rspb.2006.0005)

Svetlichnyy, L. S. 1987 Speed, force and energy expenditure in the movement of copepods. *Oceanology* **27**, 497–502.

Svetlichny, L. S. & Hubareva, E. S. 2005 The energetics of *Calanus euxinus*: locomotion, filtration of food and specific dynamic action. *J. Plankton Res.* **27**, 671–682. (doi:10.1093/plankt/fbi041)

Taylor, G. K., Nudds, R. L. & Thomas, A. L. R. 2003 Flying and swimming animals cruise at a Strouhal number tuned for high power efficiency. *Nature* **425**, 707–710. (doi:10.1038/nature02000)

Titelman, J. 2003 Swimming and escape behavior of copepod nauplii: implications for predator-prey interactions among copepods. *Mar. Ecol. Prog. Ser.* **213**, 203–213. (doi:10.3354/meps213203)

Van Duren, L. A. & Videler, J. J. 2003 Escape from viscosity: the kinematics and hydrodynamics of copepod foraging and escape swimming. *J. Exp. Biol.* **206**, 269–279. (doi:10.1242/jeb.00079)

Van Duren, L. A., Stamhuis, E. J. & Videler, J. J. 2003 Copepod feeding currents: flow patterns, filtration rates and energetics. *J. Exp. Biol.* **206**, 255–267. (doi:10.1242/jeb.00078)

Verity, P. G. & Smetacek, V. 1996 Organism life cycles, predation, and the structure of marine pelagic ecosystems. *Mar. Ecol. Prog. Ser.* **130**, 277–293. (doi:10.3354/meps130277)

Vlymen, W. J. 1970 Energy expenditure of swimming copepods. *Limnol. Oceanogr.* **15**, 348–356. (doi:10.4319/lo.1970.15.3.0348)

Waggett, R. J. & Buskey, E. J. 2007 Calanoid copepod escape behavior in response to a visual predator. *Mar. Biol.* **150**, 599–607. (doi:10.1007/s00227-006-0384-3)

Waggett, R. J. N. & Buskey, E. J. 2008 Escape reaction performance of myelinated and nonmyelinated calanoid copepods. *J. Exp. Mar. Biol. Ecol.* **361**, 111–118. (doi:10.1016/j.jembe.2008.05.006)

White, F. M. 2006 *Viscous fluid flow*, 3rd edn. New York, NY: McGraw-Hill.

Yen, J. & Strickler, J. R. 1996 Advertisement and concealment in the plankton: what makes a copepod hydrodynamically conspicuous? *Inv. Biol.* **115**, 191–205. (doi:10.2307/3226930)